

An ^{89}Zr -HDL PET Tracer Monitors Response to a CSF1R Inhibitor

Christian A. Mason¹, Susanne Kossatz¹, Lukas M. Carter¹, Giacomo Pirovano¹, Christian Brand¹, Navjot Guru¹, Carlos Pérez-Medina^{2,3}, Jason S. Lewis^{1,4,5}, Willem J.M. Mulder^{2,6–8}, and Thomas Reiner^{1,5,9,10}

¹Department of Radiology, Memorial Sloan Kettering Cancer Center, New York, New York; ²Translational and Molecular Imaging Institute, Icahn School of Medicine at Mount Sinai, New York, New York; ³Centro Nacional de Investigaciones Cardiovasculares Carlos III, Madrid, Spain; ⁴Molecular Pharmacology Program, Memorial Sloan Kettering Cancer Center, New York, New York; ⁵Department of Radiology, Weill Cornell Medical College, New York, New York; ⁶Department of Oncological Sciences, Icahn School of Medicine at Mount Sinai, New York, New York; ⁷Laboratory of Chemical Biology, Department of Biomedical Engineering and Institute for Complex Molecular Systems, Eindhoven University of Technology, Eindhoven, The Netherlands; ⁸Department of Medical Biochemistry, Amsterdam University Medical Centers, Academic Medical Center, Amsterdam, The Netherlands; ⁹Chemical Biology Program, Memorial Sloan Kettering Cancer Center, New York, New York; and ¹⁰Center for Molecular Imaging and Nanotechnology (CMINT), Memorial Sloan Kettering Cancer Center, New York, New York

The immune function within the tumor microenvironment has become a prominent therapeutic target, with tumor-associated macrophages (TAMs) playing a critical role in immune suppression. We propose an ^{89}Zr -labeled high-density lipoprotein (^{89}Zr -HDL) nanotracer as a means of monitoring response to immunotherapy.

Methods: Female MMTV-PyMT mice were treated with pexidartinib, a colony-stimulating factor 1 receptor (CSF1R) inhibitor, to reduce TAM density. The accumulation of ^{89}Zr -HDL within the tumor was assessed using PET/CT imaging and autoradiography, whereas TAM burden was determined using immunofluorescence.

Results: A significant reduction in ^{89}Zr -HDL accumulation was observed in PET/CT images, with $2.9\% \pm 0.3\%$ and $3.7\% \pm 0.2\%$ injected dose/g for the pexidartinib- and vehicle-treated mice, respectively. This reduction was corroborated *ex vivo* and correlated with decreased TAM density. **Conclusion:** These results support the potential use of ^{89}Zr -HDL nanoparticles as a PET tracer to quickly monitor the response to CSF1R inhibitors and other therapeutic strategies targeting TAMs.

Key Words: immunotherapy; tumor-associated macrophages; PET/CT imaging; CSF1R inhibitor; HDL

J Nucl Med 2020; 61:433–436

DOI: 10.2967/jnumed.119.230466

Breast cancer is the second leading cause of cancer-related death for women in the United States. Mortality in breast cancer results from the formation of metastases in organs such as the brain, liver, lungs, and bone marrow (1). Although most patients do not

present with metastatic lesions in distant tissue on initial diagnosis, 1 in 3 women with node-negative and an even larger percentage of those with node-positive breast cancer will eventually develop distant metastases (2). The standard of care for early- and late-stage breast cancers includes chemotherapy, radiation therapy, or endocrine therapy (3). Although the 5-y survival rate for breast cancer is near 90%, the rate significantly decreases to 30% in metastatic breast cancer (4). An appreciable amount of research has described the critical roles that the innate and adaptive immune system plays in cancer development and progression (5,6). Immune checkpoint blockade, engineered chimeric antigen receptor T cells, and other drugs designed to modulate the activity and migration of innate and adaptive immune cells have become focal points of preclinical and clinical research (7).

The recruitment of myeloid cells, in particular macrophages, is considered to be one of the earliest and most crucial phases in the development of metastatic lesions (2). Macrophages exhibit dual functionality in modulating immune response: classically activated macrophages are proinflammatory, whereas alternatively activated macrophages secrete cytokines that induce tissue repair and suppress immune function (8). The accumulation of macrophages within the tumor and their shift toward an alternatively activated phenotype results in signaling cascades that induce angiogenesis, alter the extracellular matrix, and suppress adaptive immune response (9–11). Therefore, tumor-associated macrophage (TAM) burden has been correlated with rapid tumor growth, metastatic potential, and poor patient prognosis (12).

Colony-stimulating factor 1 (CSF1) and its respective receptor (CSF1R) play a key role in the recruitment and activation of macrophages (13). There are numerous clinical trials exploring the use of CSF1R inhibitors as a monotherapy or in combination with other therapeutic strategies in various types of cancer (14). Pexidartinib (PLX3397), a CSF1R inhibitor currently in phase 3 clinical trials, has shown promising results as a monotherapy and in combination with immune checkpoint therapies (14). However, traditional methods of evaluating patient response can provide misleading results. Thus, physicians require approximately 3–4 mo to properly assess treatment efficacy in patients undergoing immunotherapies (15).

Received May 1, 2019; revision accepted Jul. 24, 2019.

For correspondence or reprints contact: Thomas Reiner, Memorial Sloan Kettering Cancer Center, 1275 York Ave., New York, NY 10065.

E-mail: Reinert@mskcc.org

Published online Aug. 16, 2019.

Immediate Open Access: Creative Commons Attribution 4.0 International License (CC BY) allows users to share and adapt with attribution, excluding materials credited to previous publications. License: <https://creativecommons.org/licenses/by/4.0/>. Details: <http://jnm.snmjournals.org/site/misc/permission.xhtml>.

COPYRIGHT © 2020 by the Society of Nuclear Medicine and Molecular Imaging.

The affinity of high-density lipoprotein (HDL) particles for macrophages has been well documented, and numerous formulations have been engineered to noninvasively visualize macrophage accumulation in a variety of inflammatory diseases such as atherosclerosis, arthritis, and cancers using different imaging modalities (16–20). Here, we explore the use of ^{89}Zr -labeled reconstituted HDL as a macrophage-targeted diagnostic tool that might help clinicians more quickly and accurately assess the response to anti-TAM immunotherapies. To evaluate the ability of ^{89}Zr -HDL to noninvasively monitor TAM burden by PET, we chose an aggressive transgenic mouse model of mammary adenocarcinoma: MMTV-PyMT (21). The biodistribution of ^{89}Zr -HDL nanoparticles, specifically the accumulation in the tumor, was analyzed and compared in pexidartinib-treated and untreated MMTV-PyMT mice (Supplemental Fig. 1; supplemental materials are available at <http://jnm.snmjournals.org>).

RESULTS

Synthesis and Radiolabeling of HDL Nanoparticles

^{89}Zr -labeled HDL nanoparticles were prepared following our previously reported methods (Fig. 1A) (18). Deferoxamine-HDL nanoparticles had a hydrodynamic diameter of 10.9 ± 2.8 nm ($n = 3$), as determined by DLS (Fig. 1B). ^{89}Zr -HDL nanoparticles were isolated in a $93\% \pm 6\%$ ($n = 3$) radiochemical yield and greater than 99% radiochemical purity, as determined by radio-high-performance liquid chromatography (Fig. 1C).

PET/CT Imaging and *In Vivo* Quantification of ^{89}Zr -HDL Nanoparticles

To assess the ability of the ^{89}Zr -HDL nanoparticles to act as a macrophage tracer to monitor CSF1R inhibition, MMTV-PyMT mice were treated with PLX3397 or vehicle for 5 d via daily oral gavage. This particular strain of mice begins to spontaneously develop mammary adenocarcinomas as early as 3 wk old (21). At approximately 11 wk of age, when the mammary tumors had grown to an average volume of 200 mm³, the treatment was

initiated. PLX3397 and vehicle were administered for 5 d based on previously reported results (13). The mice were then given the ^{89}Zr -HDL nanoparticles and imaged 24 h after injection. ^{89}Zr -HDL uptake in tumors, determined noninvasively by drawing volumes of interest over the entire tumor mass within the mammary glands on the PET/CT images (Supplemental Fig. 2), was significantly lower in PLX3397-treated mice than in controls ($2.9\% \pm 0.3\%$ vs. $3.7\% \pm 0.2\%$ injected dose/g, $P < 0.01$; Fig. 2B).

Ex Vivo Quantification of ^{89}Zr -HDL Nanoparticles and Macrophage Burden

The mice were euthanized by CO₂ asphyxiation immediately after PET/CT imaging, and the tumors were harvested, frozen in optimal-cutting-temperature compound, and sectioned for immunofluorescence and autoradiographic analysis. Macrophage burden was quantified through IBA-1 staining followed by immunofluorescence imaging, with observed macrophage densities of $3.1\% \pm 0.9\%$ and $12.3\% \pm 6.4\%$ IBA-1 positive cells for PLX3397- and vehicle-treated mice, respectively ($P < 0.05$; Fig. 3B). In addition, the ^{89}Zr -HDL nanoparticle accumulation was assessed using autoradiography and normalized to the injected dose. This analysis showed a significantly lower radioactivity deposition in tumors from PLX3397-treated mice than in controls (11.3 ± 1.2 vs. 15.8 ± 3.2 maximum arbitrary unit per injected dose, $P < 0.05$; Fig. 3C). The differences in nanoparticle accumulation, as observed in both *in vivo* and *ex vivo* analyses, correlate with the changes in TAM density as a result of CSF1R inhibition (22,23).

DISCUSSION

The purpose of this study was to evaluate the use of an ^{89}Zr -HDL nanoparticle as a macrophage tracer that might provide clinicians an additional tool to assess the effect of CSF1R inhibitors and other immunotherapies on TAMs. The intricate role TAMs play in altering immune function within the tumor microenvironment has made them of particular interest as targets in numerous therapeutic studies (11,14). The combination of therapeutic strategies altering both the innate and the adaptive immune system is promising; however, there are currently no accepted biomarkers that can accurately predict immunotherapy efficacy (7). Traditional methods such as RECIST can be misleading when evaluating patients undergoing immunotherapy, because tumor size can vary with changes in immune cell infiltration (15,24,25). This phenomenon, known as pseudoprogression, prevents physicians from contemporaneously assessing therapeutic responses, delaying conclusive evaluation to at least 3–4 mo after treatment initiation (26,27). Therefore, a significant clinical need exists to develop methods that can quickly and accurately monitor the effect of these therapies on TAM populations.

The observed ^{89}Zr -HDL uptake assessed through *in vivo* PET/CT and *ex vivo* autoradiography analyses showed significant differences between PLX3397- and vehicle-treated cohorts. The excised tumors included areas of high fat content, as they

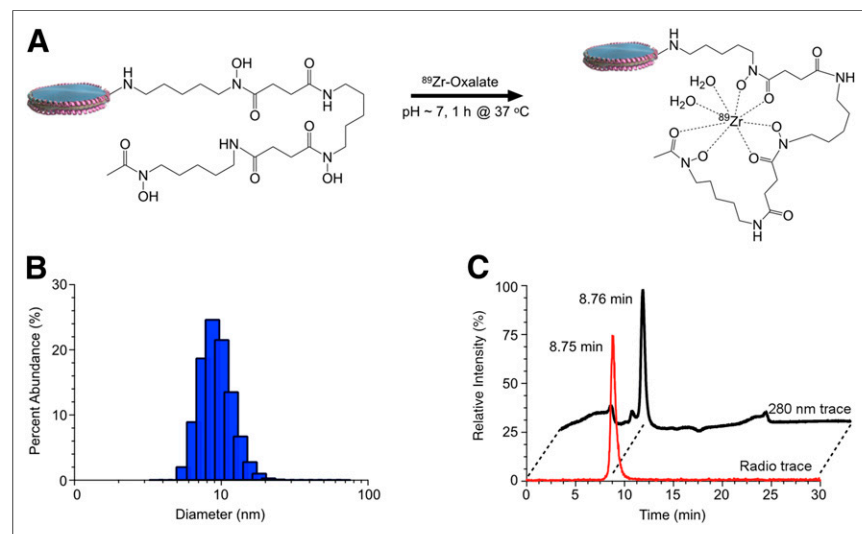


FIGURE 1. Synthesis and characterization of ^{89}Zr -HDL nanoparticles. (A) Radiolabeling synthesis conditions for formation of ^{89}Zr -HDL nanoparticles. (B) Dynamic light scattering analysis of HDL nanoparticles exposed to labeling conditions. (C) Radio-high-performance liquid chromatography analysis illustrating chemical and radiochemical purity of ^{89}Zr -HDL nanoparticles.

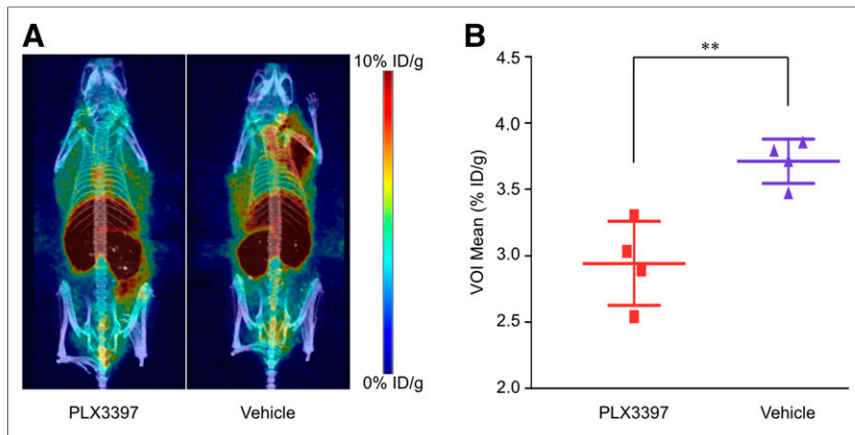


FIGURE 2. *In vivo* analysis of ^{89}Zr -HDL nanoparticles, visualized by PET/CT, showing reduced accumulation in mice treated with PLX3397. (A) PET/CT images representing ^{89}Zr -HDL nanoparticle distribution. (B) Quantification of ^{89}Zr -HDL nanoparticle uptake determined by drawing volume of interest (VOI) over entire tumor burden. ID = injected dose. $^{**}P < 0.01$.

were collected from the mammary fat pad, making it difficult to draw regions of interest that included only the cancer cells and stroma. When the activity was averaged over the drawn region of interest, a decrease in nanoparticle accumulation as a result of PLX3397 treatment was observed (Supplemental Fig. 3B). However, the differences in accumulation between the two groups were not statistically significant. Thus, the maximum accumulated activity within each tissue section was also analyzed to reduce the impact of areas with high fat content and very low nanoparticle accumulation on the analysis. The resulting data for the excised tumors showed statistically significant differences in ^{89}Zr -HDL

nanoparticles between the two cohorts (Fig. 3C). The immunofluorescence analysis provided evidence of effective reduction in macrophage density within the tumor as a result of the CSF1R inhibition. In addition, whereas IBA-1 is a prominently used macrophage stain in immunofluorescence, its expression is not exclusive to macrophages (28). IBA-1 can also appear on other myeloid cells such as monocytes and some lymphocytes. CSF1R inhibition, using PLX3397, was shown to be ineffective at reducing infiltration of monocytes and dendritic cells in the MMTV-PyMT mouse model (13). Thus, any IBA-1 staining associated with these cell populations may have led to smaller observed differences in TAM populations between the PLX3397- and vehicle- treated cohorts (13). Although there was considerable variation in TAM density between tissue sections, illustrating the highly heterogeneous nature of the tumor microenvironment, the differences between the PLX3397- and vehicle-treated cohorts remained statistically significant (Fig. 3B). A correlation between macrophage density and ^{89}Zr -HDL nanoparticle accumulation was observed in both the PET/CT and the *ex vivo* analyses (Supplemental Fig. 3). As is apparent in the PET/CT images, there was significant accumulation of the ^{89}Zr -HDL nanoparticles within the liver (Fig. 2A). Thus, whereas the tracer is ostensibly capable of imaging tumors in most tissues, the ^{89}Zr -HDL nanoparticles would likely be unable to delineate metastases within the liver. The observed differences in nanoparticle accumulation, assessed using both *in vivo* PET/CT imaging and *ex vivo* autoradiography, were the result of modulations in TAM density as a consequence of treatment with the CSF1R inhibitor, pexidartinib. As observed in the *ex vivo* analysis, the macrophage content and nanoparticle accumulation was very heterogeneous. The use of PET/CT was able to overcome this heterogeneity, as ^{89}Zr -HDL nanoparticle accumulation provided a quantifiable means of evaluating TAM content over the entire tumor area. Thus, the use of ^{89}Zr -HDL nanoparticles as a macrophage-avid PET tracer provides a noninvasive tool to quantitatively assess overall macrophage burden and could provide clinicians the means to quickly and accurately assess response to macrophage-targeted therapies.

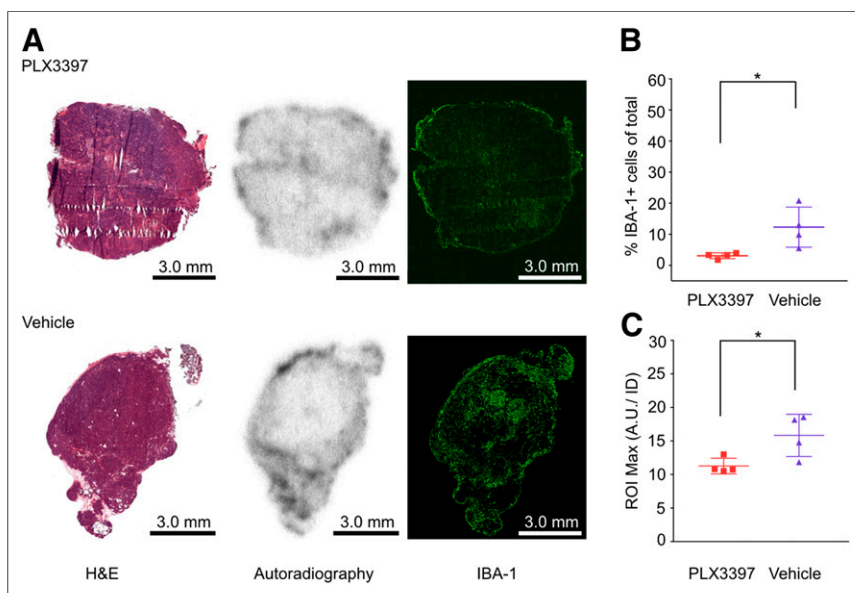


FIGURE 3. *Ex vivo* quantification of ^{89}Zr -HDL nanoparticles correlates with tumor-associated macrophage density. (A) Hematoxylin and eosin (H&E), autoradiography, and immunofluorescence images of tumors excised from MMTV-PyMT mice. (B) Quantification of TAMs represented as percentage of total cells. (C) Maximum accumulation of ^{89}Zr -HDL nanoparticles within region of interest (ROI) on autoradiography; activity was normalized to injected dose for each mouse. A.U./ID = arbitrary unit per injected dose. $^{*}P < 0.05$.

CONCLUSION

The data presented herein show that ^{89}Zr -HDL tumor uptake correlates with macrophage density within the tumor microenvironment. The statistically significant modulation in TAM burden, as a result of PLX3397 treatment, could be observed by quantifiable differences in ^{89}Zr -HDL nanoparticle uptake using PET imaging within 1 wk of initiating treatment. Thus, ^{89}Zr -HDL

nanoparticles are a promising tool that could potentially help physicians more rapidly and accurately determine the early response to therapies targeting the immunosuppressed tumor microenvironment.

DISCLOSURE

This work was supported by the MSK Molecularly Targeted Intraoperative Imaging Fund, the Tow foundation, and National Institutes of Health grants R35 CA232130, R01 CA204441, P30 CA008748, R01 CA220234, and F32-EB025050. No other potential conflict of interest relevant to this article was reported.

ACKNOWLEDGMENTS

We thank the Small Animal Imaging Core, Radiochemistry and Molecular Imaging Probes Core, Molecular Cytology Core, Center for Molecular Imaging and Nanotechnology (CMINT), Imaging and Radiation Sciences Program.

KEY POINTS

QUESTION: Is it possible to utilize a macrophage-selective ⁸⁹Zr-HDL nanoparticle as a PET imaging agent to monitor the response to a CSF1R inhibitor?

PERTINENT FINDINGS: In a murine breast cancer model we observed significant differences in ⁸⁹Zr-HDL nanoparticle uptake with 3.7 ± 0.2 %ID/g and 2.9 ± 0.3 %ID/g for the vehicle- and pexidartinib-treated mice, respectively. This reduction in nanoparticle uptake correlated with decreased tumor-associated macrophages as a result of CSF1R inhibition.

IMPLICATIONS FOR PATIENT CARE: The results in this manuscript provide evidence supporting the possible translation of the ⁸⁹Zr-HDL nanoparticles as a means of monitoring CSFR1 inhibition and potentially other therapeutic strategies that modulate tumor-associated macrophage activity.

REFERENCES

- Guo F, Kuo Y, Shih YCT, Giordano SH, Berenson AB. Trends in breast cancer mortality by stage at diagnosis among young women in the United States. *Cancer*. 2018;124:3500–3509.
- Kimbung S, Loman N, Hedenfalk I. Clinical and molecular complexity of breast cancer metastases. *Semin Cancer Biol*. 2015;35:85–95.
- Treatment of stage IV (metastatic) breast cancer. American Cancer Society website. <https://www.cancer.org/cancer/breast-cancer/treatment/treatment-of-breast-cancer-by-stage/treatment-of-stage-iv-advanced-breast-cancer.html>. Revised May 31, 2019. Accessed September 12, 2019.
- Cancer stat facts: female breast cancer. Surveillance, Epidemiology, and End Results Program website. <https://seer.cancer.gov/statfacts/html/breast.html>. Accessed September 12, 2019.
- de Visser KE, Eichten A, Coussens LM. Paradoxical roles of the immune system during cancer development. *Nat Rev Cancer*. 2006;6:24–37.
- Marx J. Inflammation and cancer: the link grows stronger—research into a long-suspected association between chronic inflammation and cancer reveals how the immune system may be abetting tumors. *Science*. 2004;306:966–968.
- Havel JJ, Chowell D, Chan TA. The evolving landscape of biomarkers for checkpoint inhibitor immunotherapy. *Nat Rev Cancer*. 2019;19:133–150.
- Murray PJ. Macrophage polarization. *Annu Rev Physiol*. 2017;79:541–566.
- Marelli G, Allavena P, Erreni M. Tumor-associated macrophages, multi-tasking cells in the cancer landscape. *Cancer Res Front*. 2015;1:149–161.
- Chamsee T, Ontong P, Konno K, Itano N. Tumor-associated macrophages as major players in the tumor microenvironment. *Cancers (Basel)*. 2014;6:1670–1690.
- Williams CB, Yeh ES, Soloff AC. Tumor-associated macrophages: unwitting accomplices in breast cancer malignancy. *NPJ Breast Cancer*. 2016;2:15025.
- Zhao X, Qu J, Sun Y, et al. Prognostic significance of tumor-associated macrophages in breast cancer: a meta-analysis of the literature. *Oncotarget*. 2017;8:30576–30586.
- DeNardo DG, Brennan DJ, Rexhepaj E, et al. Leukocyte complexity predicts breast cancer survival and functionally regulates response to chemotherapy. *Cancer Discov*. 2011;1:54–67.
- Cannarile MA, Weisser M, Jacob W, Jegg A-M, Ries CH, Rüttinger D. Colony-stimulating factor 1 receptor (CSF1R) inhibitors in cancer therapy. *J Immunother Cancer*. 2017;5:53.
- Hodi FS, Ballinger M, Lyons B, et al. Immune-Modified Response Evaluation Criteria In Solid Tumors (imRECIST): refining guidelines to assess the clinical benefit of cancer immunotherapy. *J Clin Oncol*. 2018;36:850–858.
- Mulder WJM, Strijkers GJ, van Tilborg GAF, Griffioen AW, Nicolay K. Lipid-based nanoparticles for contrast-enhanced MRI and molecular imaging. *NMR Biomed*. 2006;19:142–164.
- Cormode DP, Jarzyna PA, Mulder WJM, Fayad ZA. Modified natural nanoparticles as contrast agents for medical imaging. *Adv Drug Deliv Rev*. 2010;62:329–338.
- Pérez-Medina C, Tang J, Abdel-Atti D, et al. PET imaging of tumor-associated macrophages with ⁸⁹Zr-labeled high-density lipoprotein nanoparticles. *J Nucl Med*. 2015;56:1272–1277.
- Pérez-Medina C, Binderup T, Lobatto ME, et al. In vivo pet imaging of HDL in multiple atherosclerosis models. *JACC Cardiovasc Imaging*. 2016;9:950–961.
- Weissleder R, Nahrendorf M, Pittet MJ. Imaging macrophages with nanoparticles. *Nat Mater*. 2014;13:125–138.
- Guy CT, Cardiff RD, Muller WJ. Induction of mammary tumors by expression of polyomavirus middle T oncogene: a transgenic mouse model for metastatic disease. *Mol Cell Biol*. 1992;12:954–961.
- Strachan DC, Ruffell B, Oei Y, et al. CSF1R inhibition delays cervical and mammary tumor growth in murine models by attenuating the turnover of tumor-associated macrophages and enhancing infiltration by CD8+ T cells. *Oncimmunology*. 2013;2:e26968.
- Stanley ER, Chitu V. CSF-1 receptor signaling in myeloid cells. *Cold Spring Harb Perspect Biol*. 2014;6:a021857.
- Romano E, Schwartz GK, Chapman PB, Wolchock JD, Carvajal RD. Treatment implications of the emerging molecular classification system for melanoma. *Lancet Oncol*. 2011;12:913–922.
- Hodi FS, Hwu W-J, Kefford R, et al. Evaluation of immune-related response criteria and RECIST v1.1 in patients with advanced melanoma treated with pembrolizumab. *J Clin Oncol*. 2016;34:1510–1517.
- Schwartz LH, Litière S, de Vries E, et al. RECIST 1.1: update and clarification—from the RECIST committee. *Eur J Cancer*. 2016;62:132–137.
- Tazdait M, Mezquita L, Lahmar J, et al. Patterns of responses in metastatic NSCLC during PD-1 or PDL-1 inhibitor therapy: comparison of RECIST 1.1, irRECIST and iRECIST criteria. *Eur J Cancer*. 2018;88:38–47.
- Kanazawa H, Ohsawa K, Sasaki Y, Kohsaka S, Imai Y. Macrophage/microglia-specific protein Iba1 enhances membrane ruffling and Rac Activation via phospholipase C-γ-dependent pathway. *J Biol Chem*. 2002;277:20026–20032.



The Journal of
NUCLEAR MEDICINE

An ^{89}Zr -HDL PET Tracer Monitors Response to a CSF1R Inhibitor

Christian A. Mason, Susanne Kossatz, Lukas M. Carter, Giacomo Pirovano, Christian Brand, Navjot Guru, Carlos Pérez-Medina, Jason S. Lewis, Willem J.M. Mulder and Thomas Reiner

J Nucl Med. 2020;61:433-436.

Published online: August 16, 2019.

Doi: 10.2967/jnumed.119.230466

This article and updated information are available at:
<http://jnm.snmjournals.org/content/61/3/433>

Information about reproducing figures, tables, or other portions of this article can be found online at:
<http://jnm.snmjournals.org/site/misc/permission.xhtml>

Information about subscriptions to JNM can be found at:
<http://jnm.snmjournals.org/site/subscriptions/online.xhtml>

The Journal of Nuclear Medicine is published monthly.
SNMMI | Society of Nuclear Medicine and Molecular Imaging
1850 Samuel Morse Drive, Reston, VA 20190.
(Print ISSN: 0161-5505, Online ISSN: 2159-662X)

© Copyright 2020 SNMMI; all rights reserved.